

# Nuclear quantum optics with x-ray laser pulses

Thomas J. Bürvenich,<sup>\*</sup> Jörg Evers,<sup>†</sup> and Christoph H. Keitel<sup>‡</sup>

*Max-Planck-Institut für Kernphysik, Saupfercheckweg 1, 69117 Heidelberg, Germany*

(Dated: May 17, 2018)

The direct interaction of nuclei with super-intense laser fields is studied. We show that present and upcoming high-frequency laser facilities, especially together with a moderate acceleration of the target nuclei to match photon and transition frequency, do allow for resonant laser-nucleus interaction. These direct interactions may be utilized for the model-independent optical measurement of nuclear properties such as the transition frequency and the dipole moment, thus opening the field of nuclear quantum optics. As ultimate goal, one may hope that direct laser-nucleus interactions could become a versatile tool to enhance preparation, control and detection in nuclear physics.

PACS numbers: 21.10.-k, 21.10.Re, 42.50.-p, 42.55.Vc

At present, laser-nuclear physics usually involves secondary particles such as electrons in a plasma [1]. This indirect technique allows to reach field strengths that can induce various high-energy processes such as nuclear fusion and fission or particle acceleration [2]. On the other hand, especially quantum optics demonstrates that the direct interaction of laser fields with atoms enables one to modify or even control the atomic dynamics, with a multitude of applications [3, 4]. Thus the question arises, whether direct interactions with super-intense laser fields could also be employed in nuclear physics. While the coupling of electric and nuclear transitions has been studied before [5], direct laser-nucleus interactions traditionally have been dismissed. Mostly, this was based on too small interaction matrix elements [6]. Some exceptions are the interaction of x-ray laser fields with nuclei in relation to  $\beta$  decay [7] and x-ray-driven gamma emission of nuclei [8]. With the advent of new coherent x-ray laser sources in the near future, however, these conclusions have to be reconsidered.

Therefore in this Letter, we demonstrate that currently envisaged high-frequency lasing and ion accelerator technology does allow for the direct resonant interaction of laser fields with nuclei. Besides the proof of principle, these interactions may be utilized e.g. for the optical measurement of nuclear properties such as transition frequency and dipole moment, thus opening the field of nuclear quantum optics. As an explicit example, we show that nuclei may be prepared in excited states in a controlled manner allowing for the study of nuclear reactions with excited nuclei. The time evolution of this process allows to extract nuclear parameters such as transition dipole moments free of nuclear model assumptions. We discuss requirements and limitations, as well as possible observables and applications. A key advantage of coherent x-ray laser light is that it, in principle, allows to study phenomena well known from atomic systems such as photon echos, coherent trapping or electromagnetic induced transparency [3]. This depends on the nuclear excitation spectra, and considerably increases the demands on the employed light source and target preparation. As ultimate

goal, one may hope that direct laser-nucleus interactions could become a versatile tool to enhance preparation, control and detection in nuclear physics.

Nuclei throughout the nuclear chart exhibit various kinds of excitations. The most prominent and simple ones in terms of theoretical understanding are probably (quadrupole-type) vibrations in even-even spherical systems and rotations in even-even deformed nuclei. However, depending on the nuclear system, quite complicated excitations and couplings between them can arise. Many actinide nuclei possess rather low (collective) E1 excitations [11]. These E1 transitions can be found, e.g., in alternating parity rotating bands. They are related to the collective potential of these nuclei and the interplay between quadrupole and octupole degrees of freedom in this area of the nuclear chart. But also other nuclei have E1 transitions with similar properties, hence the physics described here is not limited to a few special cases. Some example transitions are listed in Tab. I. We focus on transitions starting from metastable ground states, but transitions between excited states could be studied as well even though they are harder to prepare.

We consider the nucleus as a pure two-level system that can be described by the state vector  $|\psi\rangle = C_g|g\rangle + C_e|e\rangle$ , where  $|g\rangle$  denotes the nuclear ground state and  $|e\rangle$  denotes the excited state [3]. This approach is justified by the fact that even though we consider super-intense laser fields, on a nuclear scale, the induced perturbation is moderate. This allows to neglect relativistic effects and interactions beyond the electric dipole approximation, and to focus on near-resonantly driven transitions. The Gaussian laser pulse is given by  $E(t) \sin(\nu t)$ , where  $E(t)$  is the (time-dependent) electric field amplitude [12].  $\hbar\omega$  and  $\mu$  are the transition energy and the dipole moment, and  $\nu$  is the frequency of the laser. The Rabi frequency is given by  $\Omega(t) = \mu E(t)/\hbar$ . The time evolution of the nuclear transition under the influence of the laser field pulse can conveniently be described via a master equation treatment for the system density matrix  $\rho$ , which allows to consider additional dephasing rates for the nuclear coherences. This is required, as most high-

nucleus	transition	$\Delta E$ [keV]	$\mu$ [e fm]	$\tau(g)$	$\tau(e)$ [ps]
$^{153}\text{Sm}$	$3/2^- \rightarrow 3/2^+$	35.8	$> 0.75^{(1)}$	47 h	$< 100$
$^{181}\text{Ta}$	$9/2^- \rightarrow 7/2^+$	6.2	$0.04^{(1)}$	stable	$6 \cdot 10^6$
$^{225}\text{Ac}$	$3/2^+ \rightarrow 3/2^-$	40.1	$0.24^{(1)}$	10.0 d	720
$^{223}\text{Ra}$	$3/2^- \rightarrow 3/2^+$	50.1	0.12	11.435 d	730
$^{227}\text{Th}$	$3/2^- \rightarrow 1/2^+$	37.9	$_{-2}^{(2)}$	18.68 d	$_{-2}^{(2)}$
$^{231}\text{Th}$	$5/2^- \rightarrow 5/2^+$	186	0.017	25.52 h	1030

TABLE I: Parameters of few relevant nuclear systems and E1 transitions [11]. The transitional energy, the dipole moment, and the life times of the ground and excited state are denoted by  $\Delta E$ ,  $\mu$ ,  $\tau(g)$ , and  $\tau(e)$ , respectively. Dipole moments with super-index 1) are estimated via the Einstein A coefficient from  $\tau(e)$  and  $\Delta E$ ; values with index 2) are not listed in [11].

frequency laser facilities suffer from a limited coherence time even within single field pulses, in contrast to typical low-intensity cw laser systems as utilized in atomic physics. In a suitable interaction picture, the master equation reads ( $A_{ij} = |i\rangle\langle j|$  for  $i, j \in \{e, g\}$ )

$$\begin{aligned} \frac{\partial \rho}{\partial t} = & \frac{i}{\hbar} [H_0, \rho] - \frac{\gamma_{SE}}{2} ([A_{eg}, A_{ge}\rho] + \text{h.c.}) \\ & - \gamma_d ([A_{ee}, A_{ee}\rho] + \text{h.c.}) , \end{aligned} \quad (1)$$

where  $H_0 = \hbar\Delta A_{ee} + \hbar\Omega(t)(A_{eg} + A_{ge})/2$  with detuning  $\Delta = \nu - \omega$ . The spontaneous emission rate from the upper level is  $\gamma_{SE}$ , and  $\gamma_d$  is an additional dephasing rate to model laser field pulses with limited coherence times. Purely coherent pulses correspond to  $\gamma_d = 0$ . We further define the inversion between the two nuclear levels, given by  $W(t) = \langle g|\rho|g\rangle - \langle e|\rho|e\rangle = |C_g|^2 - |C_e|^2$ .

We have been led by the laser specifications of current x-ray laser design reports for TESLA XFEL at DESY [9] and XRL at GSI [10], see Tab. II. Acceleration of the target ions allows to bring the laser in resonance with nuclear transitions above the maximum photon energy. This, however, demands a major experimental facility that provides both suitable x-ray laser and nuclear beams. This step may not be required for next-generation laser sources or later stages of extension of the ones discussed here. In the meantime, low-energetic transitions such as in  $^{181}\text{Ta}$  or between excited nuclear states can be studied without accelerating the target.

In the following, we work in the nuclear rest frame. Thus our treatment is independent of the particular setup, be it a powerful laser source with a resting nucleus, or an accelerated nucleus with a less powerful laser beam. In the rest frame of the nucleus (subscript  $N$ ), the Doppler shifted laboratory frame (subscript  $L$ ) electric field strength  $E$  and laser frequency  $\nu$  are given by

$$E_N = \sqrt{(1+\beta)/(1-\beta)} E_L = (1+\beta)\gamma E_L \quad (2)$$

$$\nu_N = \sqrt{(1+\beta)/(1-\beta)} \nu_L = (1+\beta)\gamma \nu_L. \quad (3)$$

Table II shows the factors  $(1+\beta)\gamma$  required to match

	$\omega_{\max}$ [eV]	$I$ [W/cm <sup>2</sup> ]	$\mathcal{B}_{\text{res}}$	$I_{\text{res}}$ [W/cm <sup>2</sup> ]
X-1	56	$10^{15}$	895	$8 \cdot 10^{20}$
X-2	90	$10^{16}$	557	$3 \cdot 10^{21}$
T	12400	$10^{16} - 10^{20}$	4	$2 \cdot 10^{17} - 2 \cdot 10^{21}$

TABLE II: Example laser configurations employed in this study.  $\omega_{\max}$  is the maximum photon energy. The lab frame intensities  $I$  depend on the focussing of the beam. The parameter sets X-1/X-2 are inspired by the GSI XRL facility, the set T by SASE 1 of TESLA XFEL at DESY.  $\mathcal{B}_{\text{res}}$  is the required factor  $(1+\beta)\gamma$  to match the nuclear rest frame laser frequency with the transition frequency in  $^{223}\text{Ra}$  (see. Tab. I).  $I_{\text{res}}$  is the laser intensity in this rest frame.

rest-frame laser frequency and the transition frequency of  $^{223}\text{Ra}$ , along with the laser intensity in this frame.

Table I lists typical transition data for nuclear systems under investigation here [11]. Note that the ground states are metastable in our context, which simplifies the preparation and acceleration of the nuclei. In several cases ( $^{153}\text{Sm}$ ,  $^{223}\text{Ra}$ ,  $^{227}\text{Th}$ ,  $^{231}\text{Th}$ ), a third level exists between the ground state and the dipole-allowed excited state. Due to a branching ratio of 100:2.6 in  $^{223}\text{Ra}$ , this system still is an excellent approximation to a pure two-level system. But in  $^{227}\text{Th}$ , the branching ratio of the E1 excited state to the two lower states (at 0 keV and 9.3 keV) is 100:96, thus forming a three-level system in  $\Lambda$ -configuration. This difference will be discussed below.

We now consider the transition in  $^{223}\text{Ra}$  as a typical example which requires moderate pre-acceleration of the nuclei. Figure 1 displays the inversion of the nuclear E1 transition in  $^{223}\text{Ra}$  for a 30 fs (FWHM) pulse and various laser intensities in the nuclear rest frame. As expected, the dynamics of the two-level system strongly depends on the laser intensity. While for the lowest intensity shown the system remains almost in the ground state ( $W \approx 1$ ), with increasing order of the intensity it is more affected until it oscillates rapidly for  $I = 10^{24}$  W/cm<sup>2</sup>. A  $\pi$  pulse that would directly transfer the system to the excited state without further oscillations can be found around  $I_\pi \approx 4 \cdot 10^{22}$  W/cm<sup>2</sup>. A series of pulses can further increase the excitation, given that the time between the pulses is of similar order or smaller than the life time of the excited nuclear state. That way, subsequent pulses will enhance the inversion, which will decrease by a smaller amount in between the pulses. Figure 2 displays such a scenario for two different intensities with a train of 6 pulses. The chosen bunch repetition time corresponds to the fundamental minimum of 770ps given in the TESLA design report [9].

Next, in Fig. 3(a), the influence of the laser field detuning is shown. The excitation probability depends sensitively on the resonance condition, which, however, may be relaxed by the bandwidth of the laser pulse.

Up to now, we have considered coherent laser field pulses. In high-frequency laser facilities, however, the co-

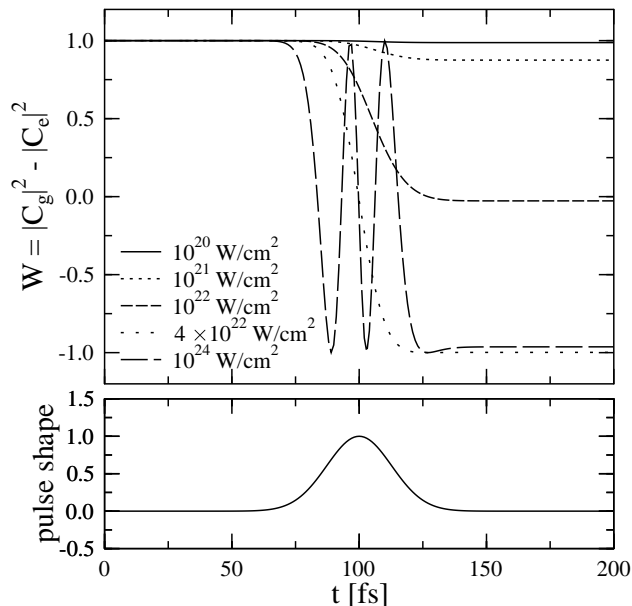


FIG. 1: Inversion  $W$  (top) and electric field envelope of the 30 fs (FWHM) Gaussian laser pulse (bottom) as functions of time in the nuclear rest frame for the E1 transition in  $^{223}\text{Ra}$ .  $|C_g|^2$  and  $|C_e|^2$  denote the occupation probabilities of the ground (g) and excited (e) state, respectively.

herence time typically is smaller than the pulse duration. We have thus added the additional cross damping rate  $\gamma_d$  in Eq. (1), which is set to values around the inverse coherence time. Results are shown in Fig. 3(b). The Rabi oscillations are damped stronger with decreasing coherence length, until the inversion  $W$  remains positive for mostly incoherent light. Note that the decrease in the inversion  $W$  can partially be countered by increasing the field intensity. Thus it is possible to observe the partial inversion with largely incoherent fields, and thus measure nuclear parameters such as the dipole moments, see below. The limited coherence implies a spectral broadening of the laser pulse, which is further increased by the finite energy resolution of the ion accelerator if acceleration is required. This decreases the number of resonant photons in the laser field, and thus leads to a reduction of the signal yield. Therefore long coherence times and high-quality beams or fixed targets are desirable, as they enhance the experimental possibilities. Note that the TESLA design report contains an extension to a two-stage FEL which would provide highly coherent light of low bandwidth with an increase in brilliance of about 500 as compared to the single-stage FEL considered here [9].

For nuclear transitions, the transitional dipole moment  $\mu$  is usually extracted with the help of the measured reduced transition probability  $B(E1; I_i \rightarrow I_f)$  [11]. The rotational model formula often used in the extraction of the dipole moment  $\mu$  is given by  $B(E1; I_i \rightarrow I_f) =$

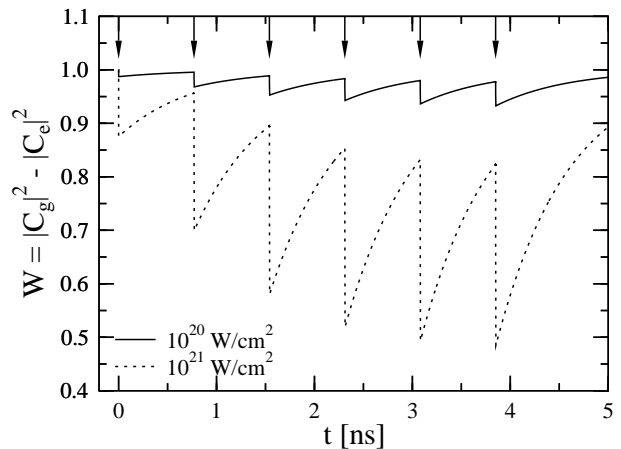


FIG. 2: Inversion  $W$  as function of time in the nuclear rest frame for the E1 transition in  $^{223}\text{Ra}$  and intensities as indicated. The maxima of the train of six 30 fs (FWHM) Gaussian laser pulses are indicated by the downward arrows.

$3/(4\pi) \times \mu^2 \times \langle I_i K_i 10 | I_f K_f \rangle^2$ . This formula involves assumptions on the structure of the nucleus, namely that the nucleus is a perfect rotator, and that the moment of inertia is identical for the levels involved. In contrast, the determination of  $\mu$  with the help of x-ray lasers constitutes an optical and more direct alternative. Measurements of the response as a function of the pulse parameters yield an excitation function from which the dipole moment can be extracted. This method is free from any assumptions on the nuclear structure but the two-level approximation, which is well justified (see Fig. 3(a)). At the same time, the dependence on the detuning could allow to measure the nuclear transition frequency. Determination of the dipole matrix element  $\mu$  via both methods provides information about the nucleus structure and the validity of the nuclear model assumptions. This will enrich our knowledge on nuclear structure and interactions between the nucleons.

The controlled excitation of nuclei with x-ray laser fields, or even nuclear Rabi oscillations, can be detected in several ways. First, fluorescence radiation is emitted during the process, which could be detected as a function of the applied field pulse. A time discrimination of the detector allows to separate between the immediate scattering and the spontaneous emission due to real excitation of the transition, and thus to avoid the primary sources of background noise, but requires fast detectors. In contrast to fixed targets and depending on the lifetime of the excited state, one could also stop and capture the accelerated nuclei, e.g., using *implementation* methods [14], or measure spontaneously emitted photons behind the interaction region rather than gating the detectors electronically. If no target acceleration is needed, then a fixed sample can be used, which may allow to

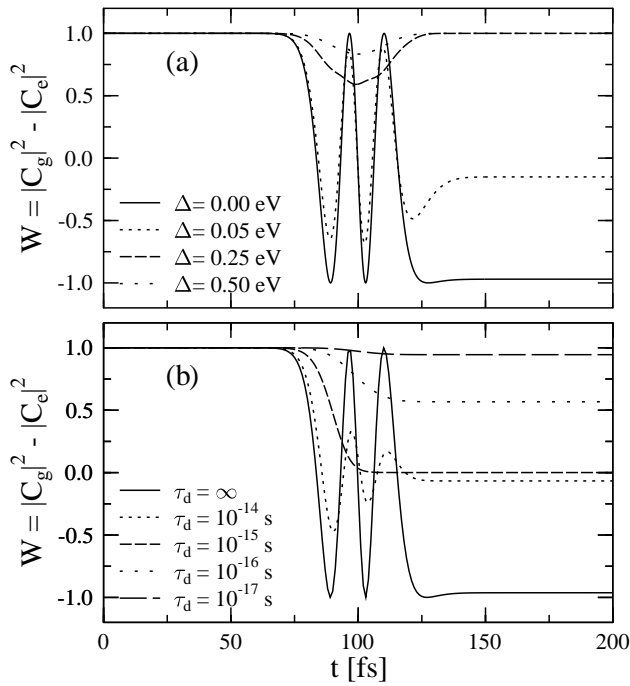


FIG. 3: Upper part (a): Inversion  $W$  versus laser field detuning in  $^{223}\text{Ra}$  for a 30 fs (FWHM) Gaussian laser pulse. Lower part (b): The inversion for different decoherence times. Both cases correspond to  $I = 10^{24} \text{ W/cm}^2$ .

increase the target particle density and thus the signal yield. From the design report for SASE 1 at TESLA XFEL and parameters for current and future ion beam sources [13], the signal rate due to spontaneous emission after real excitations of the nuclei can be estimated. For nuclei accelerated with an energy resolution of 0.1% such that 12.4 keV photons produced by SASE 1 become resonant with the E1 transition in  $^{223}\text{Ra}$ , the total photon energy spread in the nuclear rest frame is about 67 eV. From the peak photon brilliance one may estimate a flux of approx.  $4.1 \times 10^{18}$  photons/second resonant within the transition width of the excited state. Assuming in the lab frame a focal diameter of  $20 \mu\text{m}$ , focal length of twice the Rayleigh length, and laser pulse duration of 100fs, then the signal photon yield per laser pulse per single target nucleus is about  $5.4 \times 10^{-10}$ . This amounts to a signal of about 1.4 emitted photons per day for a single nucleus. With  $2.5 \times 10^{10}$  particles in a bunch length of  $\tau = 50\text{ns}$  in an ion beam of 2mm diameter as target [13] (particle density  $5.3 \times 10^8 \text{ cm}^{-3}$ ), one estimates  $2.6 \times 10^{-4}$  signal photons per pulse and  $6.8 \times 10^5$  photons per day. For a second set of parameters labelled SIS100/FAIR in [13] with particle density  $10^{11} \text{ cm}^{-3}$ , one finds  $5.3 \times 10^{-2}$  signal photons per pulse and  $1.4 \cdot 10^8$  photons per day. Note, however, that the photons per day assume a matching of ion and laser pulse repetition rate.

A second measurement principle involves nuclear state

detection, which requires a dependence of secondary processes on the internal state of the nucleus. Similar techniques are used in atomic physics, if the detection of signal photons e.g. over a thermal background is difficult [15]. The state detection methods could also be possible via *nuclear shelving*, similar to the electron shelving in atomic physics [16]. For example, the excited  $^{227}\text{Th}$  nucleus has a high branching ratio to a second metastable lower level. Thus a repeated excitation of the nucleus, e.g. in an ion storage ring, would provide selective optical pumping between the two metastable lower states, which could be detected in a subsequent secondary process without the need for fast detector gating.

TJB thanks C. Müller and U. D. Jentschura for helpful discussions.

\* Electronic address: buervenich@fias.uni-frankfurt.de;  
New address: Frankfurt Institute for Advanced Studies,  
Max-von-Laue-Str. 1, 60438 Frankfurt, Germany

† Electronic address: joerg.evers@mpi-hd.mpg.de

‡ Electronic address: keitel@mpi-hd.mpg.de

- [1] G. Pretzler *et al.*, Phys. Rev. E **58**, 1165 (1998); K. W. D. Ledingham *et al.*, Phys. Rev. Lett. **84**, 899 (2000); H. Schwoerer *et al.*, *ibid.* **86**, 2317, (2001); N. Izumi *et al.*, Phys. Rev. E **65**, 036413 (2002).
- [2] K. Boyer, T. S. Luk, and C. K. Rhodes, Phys. Rev. Lett. **60**, 557 (1988); T. Ditmire *et al.*, Nature **398**, 489 (1999); K. W. D. Ledingham, P. McKenna and R. P. Singhal, Science **300**, 1107 (2003); A. V. Sokolov and M. Zhi, J. Mod. Opt. **51**, 2607 (2004); B. Naranjo, J. K. Gimzewski and S. Putterman, Nature **434**, 1115 (2005); V. P. Krainov, Laser Phys. Lett. **2**, 89 (2005).
- [3] M. O. Scully and M. S. Zubairy, *Quantum Optics*, Cambridge University Press (1997).
- [4] R. Neugart, Eur. Phys. J. A **15**, 35 (2002).
- [5] M. Feld, "Lasers in nuclear physics", in *Lasers in Nuclear Physics*, Ed. by C. E. Bernis and H. K. Carter; V. S. Letokhov, IOP Conf. Ser. **151**, 483 (1996); O. Kocharovskaya *et al.*, Phys. Rev. Lett. **82**, 3593 (1999); G. Kozyreff *et al.*, Phys. Rev. A **64**, 013810 (2001); Y. Rostovtsev and O. Kocharovskaya, Hyperfine Int. **135**, 233 (2001).
- [6] S. Matinyan, Phys. Rep. **298**, 199 (1998).
- [7] W. Becker *et al.*, Phys. Lett. **131B**, 16, (1983).
- [8] J.J. Carroll *et al.*, Hyperfine Int. **135**, 3 (2001).
- [9] TESLA Technical Design Report Supplement, DESY Document Nr. 2002-167 (<http://www.xfel.net>).
- [10] P. Neumayer *et al.*, Appl. Phys. B **78** (2004) 957.
- [11] A. J. Aas *et al.*, Nucl. Phys. A **654**, 499 (1999); A. J. Aas *et al.*, *ibid.* **611**, 281 (1996); Nuclear Structure and Decay Databases, <http://www.nndc.bnl.gov>.
- [12] D. Bauer and P. Mulser, Phys. Rev. A **59**, 569 (1999).
- [13] N. A. Tahiret *et al.*, Phys. Rev. Lett. **95**, 035001 (2005).
- [14] *Stopping of Heavy Ions: A Theoretical Approach*, Springer Tracts in Modern Physics, Vol. 204, Springer (2004).
- [15] J. M. Raimond *et al.*, Phys. Rev. Lett. **49**, 117 (1982); **49**, 1924 (1982).

- [16] M. B. Plenio and P. L. Knight, Rev. Mod. Phys. **70**, 101 (1998).